SCIENTIFIC Publishing Limited

Prevention and Treatment of Natural Disasters

https://ojs.ukscip.com/index.php/ptnd

Article

Overview of Circular Structures of Various Origins and Sizes in Egypt as a Contribution to Natural Hazard Data Mining Based on Remote Sensing Data and Geoinformation Systems (GIS) Analysis

Barbara Theilen-Willige *

Waldstrasse 11, Scharbeutz, 23683, Germany

* Correspondence: Barbara.Theilen-Willige@t-online.de

Received: 28 September 2023; **Accepted**: 14 December 2023; **Published**: 29 December 2023

Abstract: This study is focused on the detection and typification of circular features with different sizes, origins, and states of erosion as well as on their surrounding tectonic setting, as well as on their impact on the environment and on the occurrence of natural hazards based on different satellite data of Egypt. Sentinel 2, Landsat and ASTER images and Sentinel 1- and ALOS L-band Phased Array Synthetic Aperture Radar (PALSAR)-radar data make it possible to identify larger ring structures as well as smaller circular features like maars or sinkholes in karst areas. Evaluations of the various satellite data contribute to the systematic and standardized inventory ring structures, most of which are related to magmatic intrusions. Such an inventory is a prerequisite for hazard preparedness and should be part of natural hazard data mining integrated into a Geo Information System (GIS). Mapping traces of volcanic activities (craters, maars, cones) is essential as a contribution to land use planning. By gathering the data and integrating the knowledge of the different ring structures in standardized GIS data base one of the many steps towards hazard preparedness and adapted land use planning can be achieved. Circular features are often buried by aeolian and fluvial sediments and become only visible on radar images or on Landsat or ASTER RGB images combining thermal bands. Larger ring structures have not only an influence on groundwater flow but also on geodynamic activity (earthquakes and related secondary effects).

Keywords: circular structures; remote sensing; GIS; Egypt; natural hazards

1. Introduction

A striking phenomenon in the landscape of Egypt is the occurrence of circular structures. The origin of these circular structures is quite different. They often represent the surface expression of complex phenomena occurring at greater depths [1]. A systematic inventory of these structures is an important part of a natural hazard assessment. For example: traces of volcanic activity like craters or sinkholes in karst areas might affect the safety of infrastructure, although Egypt has a low population and infrastructure density in the major parts of the country. For natural hazard preparedness it is important to know which circular structures might considered as a risk for the land use and infrastructure.

The different traces of volcanic activity might be a risk or hindrance for land use, for example, sprinkler irrigation management within areas covered by craters, dikes, and volcanic cones. The numerous dikes along fault zones have to be considered as well [2].

Most of the ring structures are related to magmatic intrusions that happened during the past geologic history. Smaller ring structures in Egypt often represent related volcanic features like maars and explosion craters with central plugs, ring dykes or cinder cones. Some structures are buried underneath younger lithologic units and extended

https://doi.org/10.54963/ptnd.v2i2.167

aeolian covers and, thus, not visible in the field. Whenever they are surface-near, ring structures can still be detected on satellite data because of the concentric outline of the drainage pattern or ring-shaped tonal anomalies on the images. Some of them are even only identifiable on images created by the combination of thermal bands of Landsat and ASTER data due to their specific thermal inertia properties, or on radar images. The radar capability to penetrate into dry and unconsolidated sedimentary covers over 1 m deep supports the detection of ring structures.

This study is focused on the detection and typification of circular features with different sizes, origins, and states of erosion as well as on their surrounding tectonic pattern and their impact on the environment, as far as possible based on remote sensing data. There are circular structures visible on the satellite images and on morphometric maps that are not documented on available geologic maps or described in the published geologic literature. Therefore, this study aims to contribute to the systematic detection and inventory of the various kinds of ring structures.

Figure 1 provides an overview of the occurrence of ring structures in Egypt. The term ring structure is used as a neutral description of the circular appearance, not related to their origin.

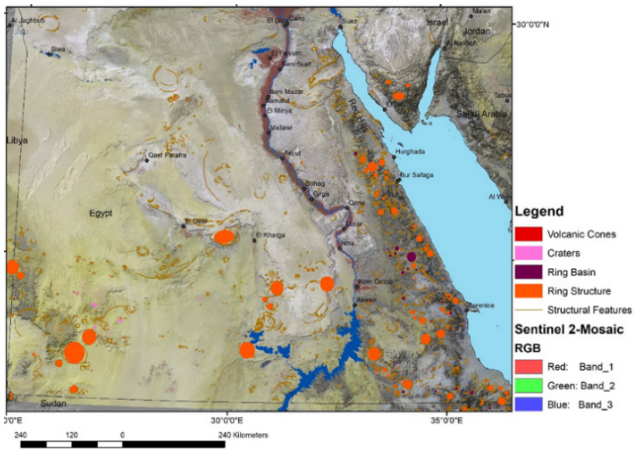

Figure 1. Ring structures in Egypt digitized based on satellite images.

Although circular or ring structures are an essential part of the landscape and of the geologic development in Egypt a systematic and standardized inventory of different types of ring structures related to their morphologic appearance, lithologic properties and ages has not been published so far. Of course, many detailed studies related to specific circular structures have been carried out such as of intrusive bodies in the Red Hills or of volcanic features in SW-Egypt or in the Western Desert [3–7].

Depending on the specific situation and purpose a detailed documentation of circular structures is important for several reasons: For hydrogeologic investigations, the knowledge about circular structures has to be considered because the groundwater flow is influenced by those structures. Concentric and radial faults and dislocations might lead to varying groundwater permeabilities. For example, they can form a hindrance to the groundwater flow and/or lead to the development of springs, depending on the specific situation.

Another reason for the detailed inventory of circular structures is the monitoring of potential geohazards: In areas with past volcanic activity unstable ground conditions can be found. Although even not recently active, the local site conditions vary considerably in volcanic areas.

Whenever stronger earthquakes happen, local site effects can influence earthquake ground motion and, then, the documented macroseismic intensity to a great deal.

Earthquake data were integrated in order to investigate if there is a relationship between surface-near geologic/tectonic structures and earthquake occurrence. Previous studies have indicated that the position of larger ring structures related to plutons with specific geomechanical properties seems to have an influence on regional earthquake occurrence and effects, such as on the macroseismic intensities [8].

Furthermore, the geothermal activity in Egypt is associated with the tectonic evolution and magmatic activities in the past. The mapping of ring structures and larger fault zones helps to identify high permeable zones that play a role as a pathway for the up-flow of hydrothermal fluids [9]. Although recent, active volcanism is not documented so far, some forms of volcanic activity (gas retreat) cannot be excluded [1,10].

Collapsing sinkholes and caves in karst areas can affect the safety of settlements and infrastructure. Thus, karst-related features like sinkholes or caves should be included in a natural hazard GIS.

2. Materials and Methods

Sentinel 1 (C-Band radar wavelength), Synthetic Aperture Radar (SAR), ALOS PALSAR (L-Band) radar data and optical Sentinel 2 images, ASTER, and Landsat 8 and 9 (Operational Land Imager-OLI) were digitally processed and evaluated. The data were provided by the USGS Earth Explorer [11], ESA Copernicus Open Access Hub [12], and NASA Earth Data, Alaska Satellite Facility (ASF) [13]. Digital image processing software served the

Sentinel Application Platform (SNAP)/ESA and ENVI/L3Harris Geospatial Solutions as well as the processing tools integrated into the geoinformation systems ArcGIS/ESRI and QGIS (Figure 2). Sentinel 2 mosaics were downloaded from the Arab Nubia Group Blog [14] and included into the data sets.

Digital image processing of Landsat TM and 8/9 (the Operational Land Imager (OLI) data was carried out by merging different Red Green Blue (RGB) band combinations. Special attention was focused on the creation of RGB images including Landsat 8/9 thermal bands 7 and 10 and ASTER thermal bands (10–14). Thermal inertia controlling surface temperatures supports the identification of ring structures. Their reflection in the thermal bands is generally quite different from the environment, depending on their mineralogic composition. The combination of the Landsat Bands 2, 7 and 10 provided a useful image base for their detection. A Landsat RGB mosaic with this band combination was created. Principal Component Analysis (PCA) was added.

High-resolution images of World Imagery files and ArcGIS Earth/ESRI and Bing Maps Aerial/Microsoft were included into the evaluations.

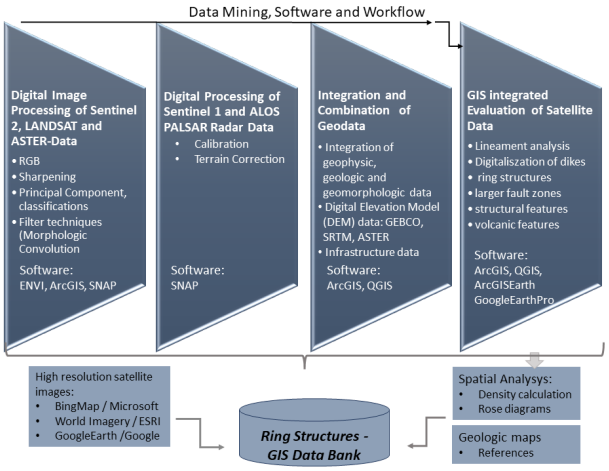

Figure 2. Workflow.

Shapefiles were created in ArcGIS related to ring structures and ring basins (without relation to their origin), volcanic features, sinkholes, lineaments (assumed to be related to fault zones), and structural features. Volcanic features, major lineaments and circular structural units were digitized visually based on the different satellite data. The larger, circular structures and the smaller circular features such as volcanic features (cinder cones, calderas, maars, impact craters) were mapped and combined in a GIS with available geologic information.

Digital Elevation Model (DEM) data and the DEM-derived morphometric maps (slope gradient, height level, curvature, drainage maps) support these investigations. Some of the larger ring structures are only visible on morphometric maps because they are traced by circular arrangements of slope gradients or by concentric drainage patterns. A weighted overlay of causal factors influencing the morphologic and geologic disposition to be affected by stronger ground motion in case of earthquakes was carried out. Based on morphometric maps and morphometric factors derived from these maps the influence of ring structures on this disposition could be partly visualized, of course, limited to the surface site conditions.

3. Geomorphologic and Geologic Overview

The topography of Egypt is characterized by different landscapes such as the Nile Delta, vast plain desert areas covered by dune fields and aeolian sand sheets, large depressions, karst landscapes within the outcrops of lime and dolostones, volcanic areas as in the SW and the Red Hills in the East along the Gulf of Suez and the Red Sea. The height level map provides an overview of the topographic situation (see Figure 3). Most of the ring structures are visible about and above height levels of about 500 m as the lower areas are covered by younger sediments. Figure 4 provides an overview of the geologic setting.

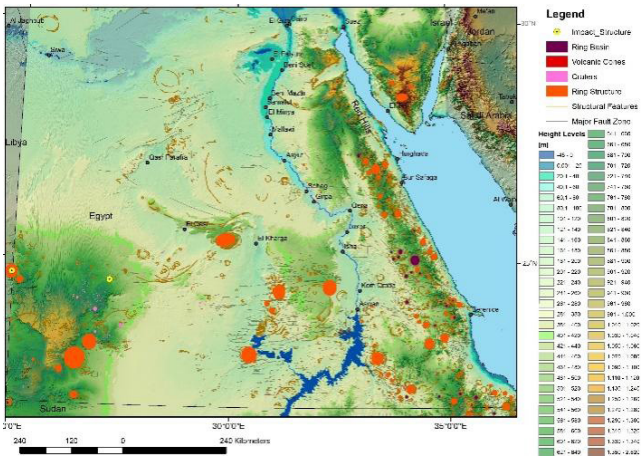

Figure 3. Height levels in Egypt derived from SRTM DEM data.

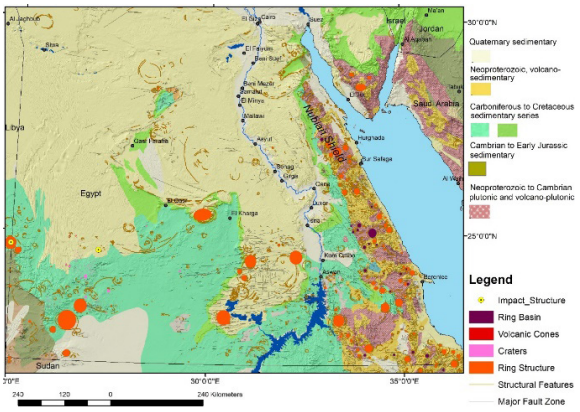

Figure 4. Geologic overview based on 1:10M-scale Geological Map of Africa-SIG Afrique—1:10,000,000 scale—Bedrock Age, French Geological Survey (BRGM), France (geologic data downloaded from the One Geology portal) [15] combined with digitized geologic features derived from satellite data.

Several hundred of the magmatic intrusions along the Red Hills were emplaced at the end of the Pan-African orogeny and the opening of the Red Sea Rift [16]. The close of the Pan-African orogeny was characterized by a change from subduction and arc-related magmatism to post-tectonic alkaline magmatism [17] comprising the emplacement of the calc-alkaline and alkaline granites at (610–590 Ma). The ring complexes can be related to swells or arches in the crust essentially distributed at random, but with some alignment along lines of weakness which might have partly existed since Precambrian times and suffered frequent rejuvenation [6]. Two major volcanic episodes have been recognized in the Neoproterozoic crust of the Arabian-Nubian Shield (an exposure of Precambrian crystalline rocks in the eastern part of Egypt). Volcanism associated with the first episode produced the 'metavolcanic' sequences including older (800–614 Ma), metamorphosed, and largely mafic rocks. This was succeeded by a younger Neoproterozoic volcanic cycle (614–550 Ma) that produced voluminous volcanic assemblages [3]. In Egypt, metavolcanic rocks are widely distributed in the central and southern parts of the Eastern Desert but are rare in the North-Eastern Desert. The rifting along the Gulf of Suez and the Egyptian Red Sea resulted in the formation of a complex, discontinuous fault pattern with very high rates of fault block rotation [18]. About 20 Ma ago tectonically driven subsidence in the Red Sea accelerated and was accompanied by an increase in denudation and uplift of the rift shoulders.

4. Evaluation Results

The occurrence of many ring structures, especially the smaller ones is related to natural hazards in the geologic past. However, they partly still have an impact on their environment, for example by influencing the local site conditions in case of stronger earthquakes. Ring structures influence the development of the fault and fracture pattern and the geodynamic movements in their environment because of their varying geomechanically properties.

The different ring structures were distinguished according to their origin, their geomorphologic appearance, lithologic composition, and size (as far as possible based on remote sensing data). Figure 5a shows a summary of the main different types and Figure 5b their sizes.

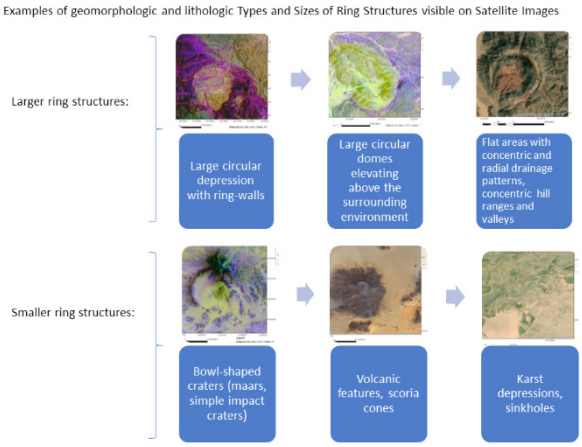

(**a**) Different types of ring structures.

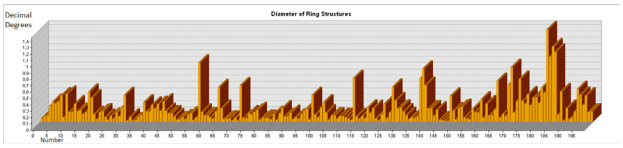

(**b**) Diameter of ring structures.

Figure 5. Overview of types and sizes of ring structures.

4.1. Ring Domes Related to Plutons

Most of the topographic positive ring structures forming hills can be related to magmatic bodies. Prominent features in the landscape are formed by larger plutons with up to more than 10 km in diameter rising above the surrounding areas as shown in the next figures. The majority of them occur in the Red Hills and are intersected by fracture and fault zones, partly with later intrusions of dikes. The circular alkaline complexes were emplaced in an intracontinental setting within the Arabian-Nubian Shield, which had been consolidated during the Pan-African orogeny (Figures 6–8) [4,15]. Figure 6 illustrates how the combination of Google Earth, Landsat 8, and SRTM DEM-derived height and

slope gradient maps support the analysis of plutons. With regard to the geodynamic movements in this area (due to rifting processes in the Red Sea and the resulting intense distortions and faulting processes in the surrounding areas) it is important to learn more about the influence of plutons on the intensity of faulting processes.

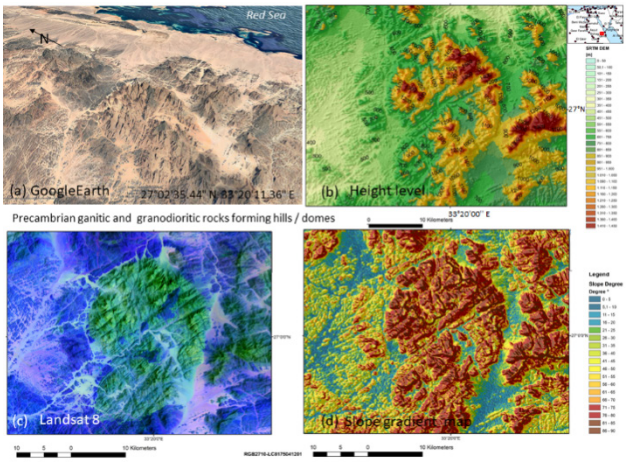

Figure 6. Precambrian granitic and granodioritic rocks forming circular hills. (**a**) Google Earth perspective view; (**b**) Height level map; (**c**) Landsat 8-scene; (**d**) Slope gradient map derived from SRTM DEM data.

An example is presented from the southern part of the Red Sea Hills. The alkaline rocks of the Gabal Shendib ring complex are composed of olivine gabbro, alkaline granite, alkaline syenite and remnants of the volcanic rocks represented by porphyritic trachyte, porphyritic rhyolite, rhyolite and associated pyroclastics. The distribution of mineralization in the alkaline rocks indicates post-magmatic hydrothermal fluids [16].

The comparative analysis of optical and radar satellite images allows a more detailed lithologic and structural assessment of the area (Figure 7). An RGB radar image was created by combining the data of the vertical (v) and horizontal (h) polarizations (RGB: vh, vv, vh). The evaluations of the different data allow a detailed structural assessment, especially of the fracture and fault pattern (Figure 7c). This knowledge is important for the understanding of later volcanic activity in this area. Along most of the Red Sea fault systems, there are local occurrences of late Cenozoic basaltic volcanism mainly due to extensional faulting, synchronously with the phase of basaltic volcanism that happened about 23 Ma, the Oligocene-Miocene transition [19]. Larger granitic domes had an influence on the occurrence of this later magmatic activity. This seems to be obvious when analyzing the dike and cinder cone distribution around larger ring structures forming larger domes. Within the dome-ring complexes, only very few dikes can be detected, whereas within ring basins and along larger shear zones around the plutons dikes are concentrated such as visible at the SE border of Egypt (Figure 8).

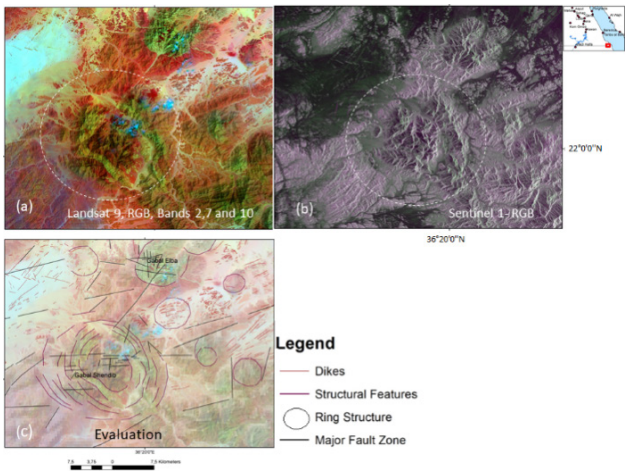

Figure 7. Comparative structural evaluation of Landsat 9 and Sentinel 1 radar images of the Shendib ring structure. (**a**) Landsat RGB scene; (**b**) Sentinel 1 radar scene; (**c**) Structural evaluation.

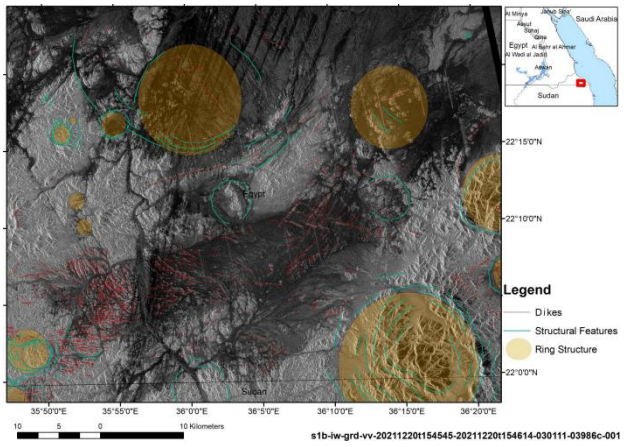

Figure 8. Evaluation of a Sentinel 1 radar scene from the SE-border of Egypt revealing larger valleys in dark tones intersected by dike swarms in the vicinity of granitic domes.

Along the Red Sea higher earthquake activity has been documented (Figure 9a) with earthquake magnitudes > 5 [18,20,21]. The seismicity is related to the interactions between the Eurasia, Africa and Arabian plates.

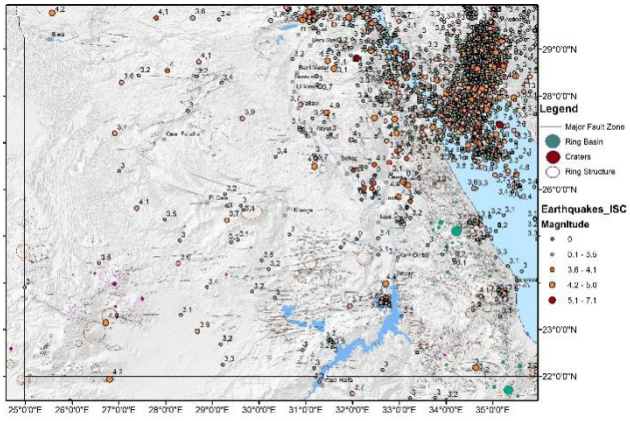

(**a**)

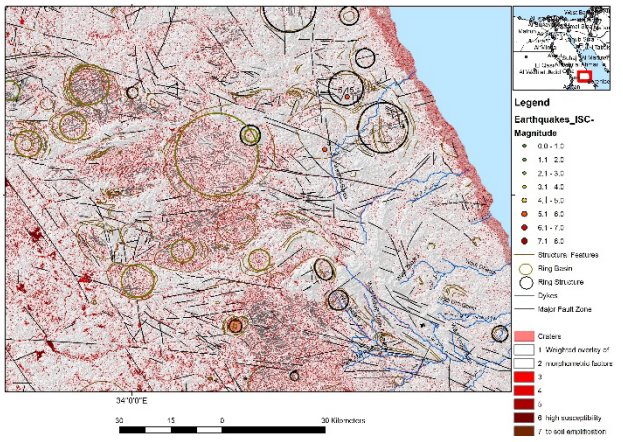

(**b**)

Figure 9. Weighted overlay result of combining and weighting geomorphologic causal factors influencing the susceptibility to higher ground motion in ArcGIS. (**a**) Earthquakes in Egypt (earthquake data: International Seismological Centre-ISC [22], US Geological Survey [23], European-Mediterranean Seismological Centre-EMSC) [24]; (**b**) Weighted overlay of causal, geomorphologic factors (low slope gradient < 10°, curvature = 0, lowest local height level, etc.) influencing the susceptibility to relatively higher ground motion in the southern Red Hills due to the geomorphologic and geologic disposition (dark-red—higher susceptibility to stronger ground motion).

Determination of region-specific ground motion is of great significance for land use planning and hazard preparedness. Assessing the influence of plutons on earthquake ground motion due to the specific surface-near geologic conditions is of importance for microzonation studies. The amplification or deamplification and lengthening of seismic ground motion has to be taken into account. Local site effects can have strong influences on the amplitude and duration of ground shaking [21]. Little is known so far about those effects in these parts of Egypt. The question arises of how the larger magmatic bodies will influence seismic wave propagation. Will they act as seismic reflectors and, thus, amplify ground motion? This might be of interest to future research.

The factors influencing the occurrence, type and intensity of earthquake induced ground motion can be separated into causal and triggering. The causal factors determine the initial conditions while the triggering factors such as high precipitation rates influence the timing. Causal factors can be derived from morphometric maps such as the slope gradient, curvature, height level, or drop raster. GIS integrated geodata analysis was used to detect and visualize some of those factors that are known to be related to the occurrence of higher earthquake shock and/or earthquake induced secondary effects: factors such as lithology (loose sedimentary covers), basin and valley topography and fault zones. The distribution of unconsolidated, youngest sedimentary covers can often be correlated with areas showing less than a 10° slope gradient and no curvature.

The susceptibility to higher ground motion is calculated by adding every layer with a weighted influence together and summing all layers. The sum of all causal factors/layers that can be included in GIS provides some information on the susceptibility to amplify seismic signals. After weighting (in %) the factors according to their probable influence on ground shaking, susceptibility maps were elaborated, where those areas were considered as being more susceptible to higher earthquake shock intensities, where "negative" factors (slope degree < 5°, height level < 100 m, curvature = 0, drop raster < 100,000) occur aggregated. The resulting maps are divided into susceptibility classes. The susceptibility to soil amplification is classified by values from 0 to 7, wherein the value 7 stands for the strongest, assumed susceptibility to soil amplification due to the aggregation of causal factors.

Ring structures forming domes show a relatively low susceptibility, whereas ring basins and depressions filled with younger sedimentary covers correlate with higher susceptibility classes. The broader valley bottoms and ring-shaped depression covered by unconsolidated sedimentary deposits will be probably more affected by earthquake shock than the areas with outcropping granitic rocks.

4.2. Ring Basins

Larger ring basins are another prominent type of circular structure in the Red Hills whenever selective erosion causes the development of depressions in the inner part of the intrusive bodies surrounded by more

resistant rock walls. Figure 10 shows an example of the southern Red Hills, where most of the larger ring basins occur concentrated. The basins are filled with loose sedimentary covers. The basins are often intersected by dikes that intruded later into the fracture and fault zones of the plutons and nowadays are visible due to their higher resistance to erosion and younger age.

Digital elevation model (DEM) data and the derived morphometric maps such as slope gradient or height level maps support the identification of circular basins.

4.3. Ring Structures Traced in Sedimentary Strata

Whereas the origin of circular structures by magmatic intrusions can be related in general relatively clearly when outcropping at the surface, it is very complex and difficult to clarify the origin of ring structures within sedimentary strata based on satellite data. Smaller ring basins and depressions within lime- and dolostones might be related to dissolution processes during more humid climate periods, see Section 4.4. Tonal anomalies on the satellite images, the drainage pattern, and subtle changes in the radar reflection on radar images can reveal circular structures in sedimentary strata that often are invisible in the field because of the flat terrains covered by aeolian sediments.

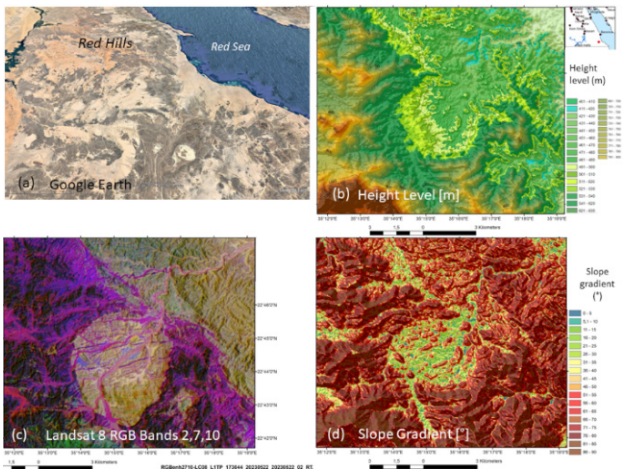

Figure 10. Ring basins. (**a**) Oblique view in Google Earth; (**b**) Height level map; (**c**) Landsat 8, RGB; (**d**) Slope gradient map in the southern Red Hills.

Whenever circular features within sedimentary layers such as sandstones, shales or limestones occur, their origin can be clarified by field investigations or geophysical data. This was not possible in the scope of this study because of financial limitations.

There might be another reason for the development of ring and oval-shaped structures as demonstrated by the following examples. These structures are situated in the SW part of the Sinn el-Kaddab plateau in the southeastern part of the Western Desert of Egypt with outcropping Tertiary shales, lime-, dolo- and sandstones that have been exposed to intense tectonic movements. The Sinn el-Kaddab plateau is a flat-topped plateau, about 300 m above the Nile Valley and Kharga Valley to the east and west respectively, and about 200 m above the Nubian Plain to the south [6]. Prominent E-W striking strike-slip faults intersect this area (especially the oval and circular shaped structures), which are tens to hundreds of kilometers long and cut bedrocks of Eocene in age.

The movements along the major fault zones might have led as well to rotations, obviously causing the development of circular and oval-shaped structures in the southern Sinn el-Kaddab Plateau (Figure 11). Carbonate hosted faults are often prone under stress to fluid-assisted pressure solution transfer that could have supported those deformation and rotation processes.

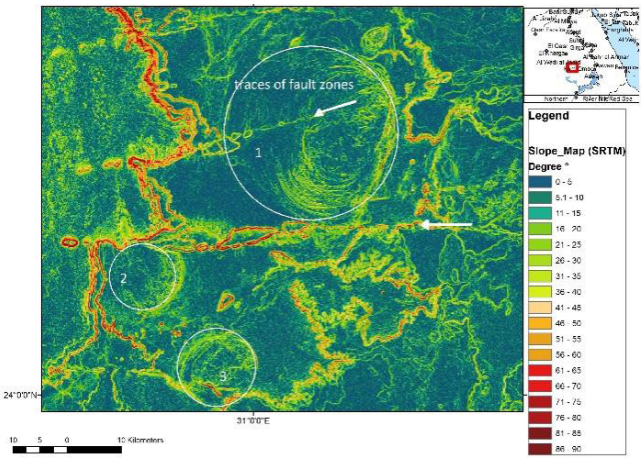

Figure 11. Slope gradient map of circular and oval-shaped structures (1–3) along faults (white arrows).

The oval-shaped structure in Figure 11 is cut in the middle by a distinct expressed SW-NE striking fault zone and in the south by a W-E oriented fault zone. Fault zones appear due to distinct steeper scarps, pull-apart depressions and push-up ridges. Figure 12a,b show the circular feature (as indicated in Figure 11, 1) on a Landsat scene combining the thermal bands. Slope gradient maps reveal that the faults have well-marked lines in the morphology. Circular structures are clearly visible on the SRTM DEM-derived slope gradient map in the SW of the Sinn el Kaddab-Plateau (Figure 12c) as well as larger fault zones. The height level map (Figure 12d) indicates the flat, tabular area.

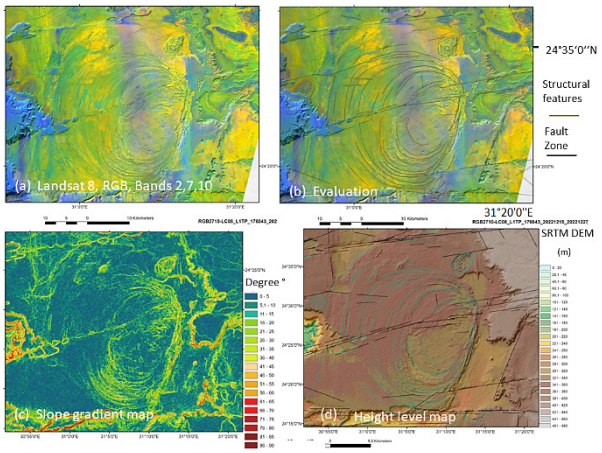

Figure 12. Oval-shaped structure within Tertiary sedimentary layers (shales, limestones, etc.) intersected by strike-slip faults. (**a**) Landsat 8-scene; (**b**) Evaluation; (**c**) Slope gradient map; (**d**) Height level map and major fault zones (black lines).

High resolution satellite imageries reveal detailed features of this fault system, including complex fault geometries that are well-exposed due to lack of vegetation and surficial cover, among these hundreds of unusual eye-shaped structures co-located with faults [6,7]. Positive and negative flower structures, en echelon faults and Riedel shear zones associated with movements along the major, W-E-striking strike-slip faults, can be observed. The origin of this oval-shaped structure embedded in limestones is in research. Whether it was created by up-doming of the strata or by rotation movements between larger, active fault zones or other reasons still has to be investigated.

Geodetic data would clarify if there are not only horizontal, but also vertical movements. Precise geodetic data providing information about the movements in this area would be helpful in investigating the intensity of fault movements and detecting whether there are local uplifts within the ring structures. In the case of active movements, not only the intensity, but also the velocity should be known.

Earthquakes were documented along these W-E oriented faults [20] indicating geodynamic activity.

A "heart-shaped", larger circular structure with a diameter of nearly 30 km developed in is shown in the next example (Figure 13). The origin of this feature like in the previous case still has to be investigated. The recent appearance was modeled by erosion.

Movements along fault zones can cause damage such as along streets, highways or irrigation systems. Thus, their mapping and monitoring should be part of a natural geohazard data bank, especially when causing rotational movements.

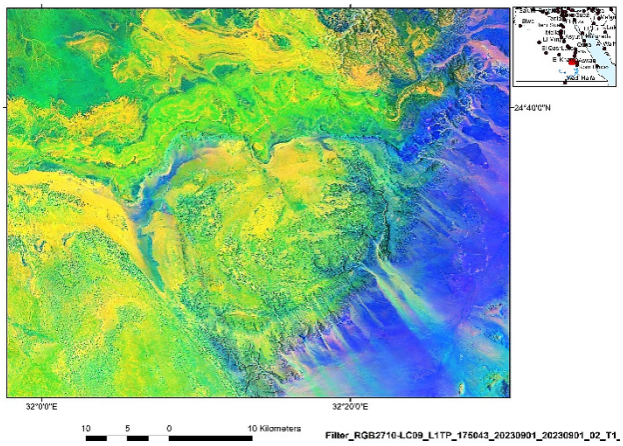

Figure 13. Traces of a circular structure in Tertiary sedimentary strata visible on a Landsat 9-scene.

During the last decades, a lot of efforts have been undertaken to extend the areas for agriculture in the Western Desert of Egypt using sprinkler irrigation (Figure 14). If there are horizontal or vertical, especially uplifting movements, this could affect the sprinkler water management because of changing water flow conditions. Traces of volcanic activity like craters and dikes are visible on satellite images surrounding this area shown in Figure 14. However, underneath the aeolian covers might be buried further volcanic features and faults.

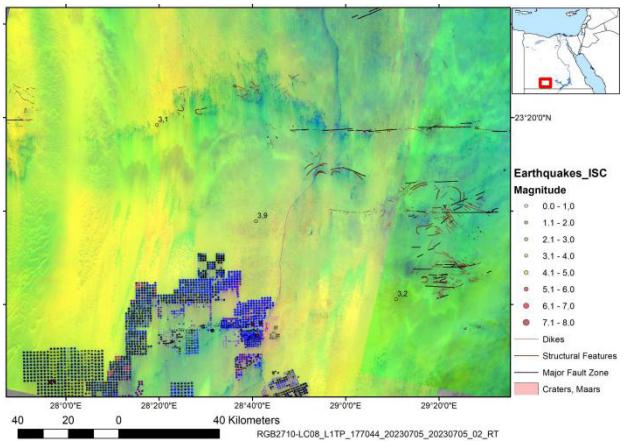

Figure 14. Landsat8-scene (RGB of thermal bands) of an agricultural site with sprinkler irrigation combined with digitized lineaments and earthquake data.

4.4. Ring Structures of volcanic Origin

Scattered surface lava flows, monogenetic cones, explosive craters, plugs, and associated dikes [1] are covering especially in the SW of Egypt. The most prominent volcanic features visible on satellite images of Egypt are the numerous craters, cinder cones, lava fields and dikes [19]. Maar diatremes resulting from magma-water interactions

produce circular and sub-circular geological structures.

As far as possible with the use of remote sensing, the different features were mapped. However, when digitizing craters based on satellite images the term "crater" refers in this study just to the morphologic description as without field work the genetic origin cannot determined.

Thermal band combinations of ASTER and Landsat data help to get additional information about areas with traces of volcanic activity. This is demonstrated by the example from SW Egypt. When evaluating an ASTER RGB combination in the visible spectrum (Figure 15c,d) only single black spots related to volcanic plugs become visible. Using the same data source but in the thermal band combination (Figure 15a,b) a larger ring structure with about 12 km in diameter appears, obviously tracing a larger magma plume underneath. Thus, additional knowledge can be gained by the digital image processing and evaluation of satellite data.

The next example presents a crater field in the Gilf Kebir volcanic province in SW-Egypt with a high density of craters. Most of the craters have a diameter of < 1 km, about 200 to 500 m (Figure 16a,b). The evaluations of Sentinel 1 (Figure 16c) and ALOS PALSAR radar data support the detection of the numerous craters even more than those of Sentinel 2 and Landsat data, often overlapping each other. On the radar images the larger, flat crater bottoms appear in dark tones, and the surrounding crater rim in light tones.

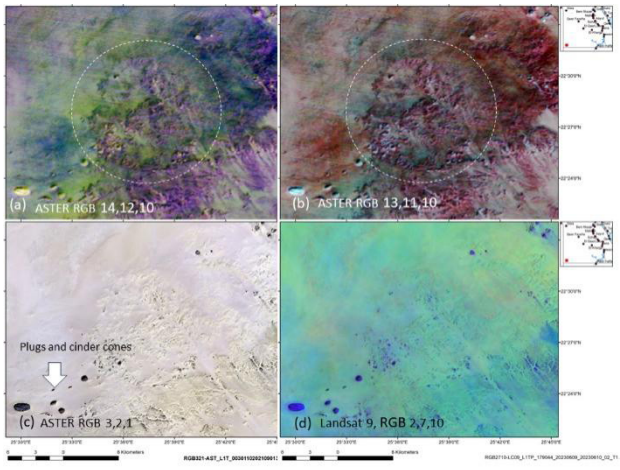

Figure 15. Traces of a larger magma plume with numerous plugs, dikes and cones visible on ASTER scenes, RGB thermal band combinations. (**a**) ASTER RGB 14,12,10; (**b**) ASTER RGB 13,11,10; (**c**) ASTER RGB 3,2,1; (**d**) Landsat 9 RGB 2,7,10.

The maars in this area are low-relief, broad volcanic craters formed by shallow explosive eruptions. The explosions must have occurred during more humid climate conditions in this area caused by the heating of groundwater when magma invaded the groundwater table. The maar craters are shallow volcanic craters with steep sides surrounded by tephra deposits. The tephra deposits are often thickest near the crater and decrease with distance from the crater [19]. A hydrothermal venting mechanism was proposed based on the fact that some of the structures are cross-cut by basaltic dikes and assumed that magmatism took place after the formation of such circular features [1].

Volcanic eruptions intersect even the large Pleistocene, N-S-oriented longitudinal dunes in SW-Egypt (Figure 17), indicating that volcanic activity has probably happened more recently in geologic time terms. The question arises whether there might be still a potential risk of volcanic eruptions. Could a stronger earthquake trigger volcanic activity? The close monitoring of these natural hazards is essential for land use planning and damage mitigation.

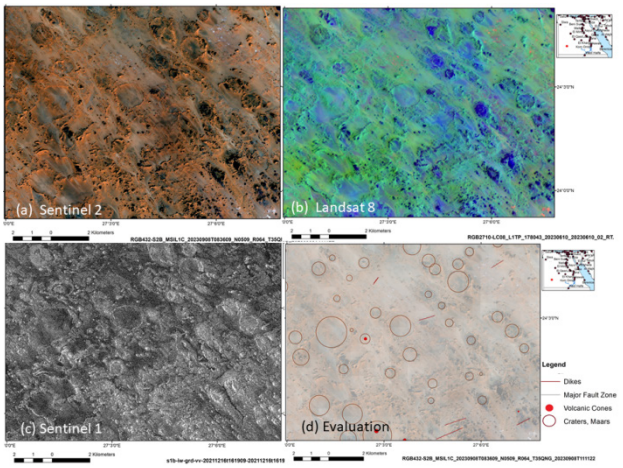

(a–d)

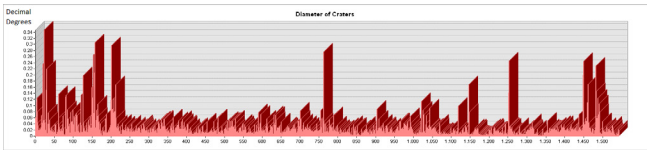

(e)

Figure 16. Crater fields in SW-Egypt. **(a)** Sentinel 2 scene; **(b)** Landsat RGB scene; **(c)** Sentinel 1 radar scene; **(d)** Digitized craters; (**e**) Diameter of craters.

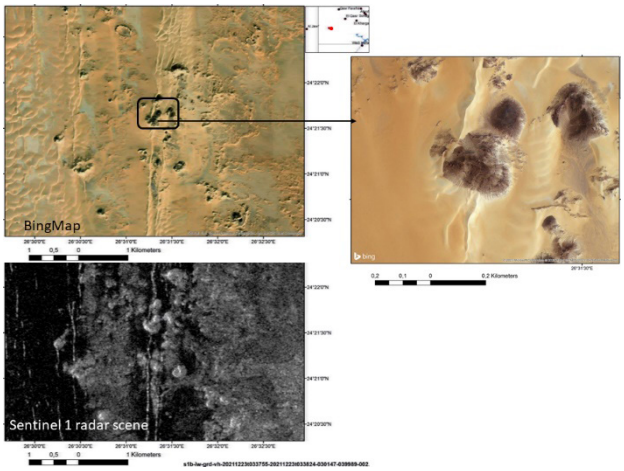

Figure 17. Traces of recent volcanism intersecting N-S oriented, longitudinal dunes in SW-Egypt.

Figure 18 shows an example of a crater with a central plug in the southern Red Hills cutting through dike swarms. Miocene magmatism, obviously linked with the opening of the Red Sea [17], resulted in surface eruptions and subsurface magmatic intrusions. In comparison with the previously shown areas in SW-Egypt, there are fewer traces of volcanic explosive activity in SE-Egypt.

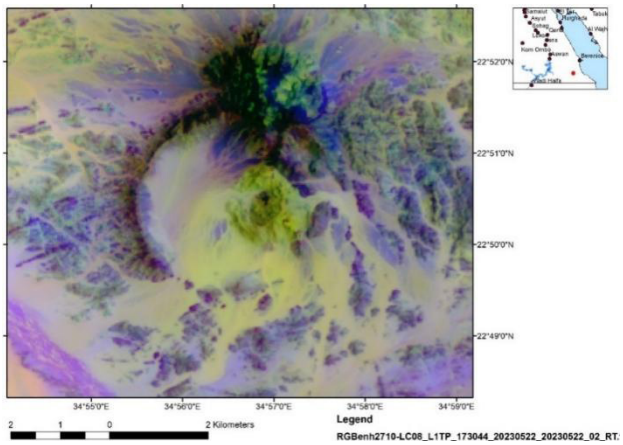

Figure 18. Crater with a central plug in the southern Red Hills.

4.5. Sinkholes in Karst Areas

Although the karst processes are the main geomorphic agents and the karst landforms are widespread all over the western plateau regions due to the presence of the Eocene carbonate rocks, most of the studies related to the geohazard assessment of palaeo-karst are still focused on selected areas so far [25–27].

Water circulation has great impacts on fractured surface areas of carbonate rocks by increasing dissolution and creating subsurface caves, sinkholes and other karst specific landforms (Figure 19). In the future, these caves can lead to ground subsidence and collapse [28,29].

Climate change with increasing extreme weather events (flash floods) will affect karst areas. Climate change is not only changing the location, frequency, and severity of environmental extremes and hazards, but also the baseline spatial and temporal patterns. More knowledge about the effects of rare flash floods on caves in Egypt is necessary. Rare intense rainfall causing flash floods in this desert climate area will affect dissolution processes in lime- and dolostones. These complex interactions need further research.

The digitization and standardized inventory of karst phenomena in the whole country is an important contribution to the geohazard management in those areas where soluble carbonates and evaporites are present at the surface and/or in the subsurface such as the area of Sohag in the west of the Nile Valley or in the Western Desert. A hazard assessment map may help in future planning for development in order to prevent damage related to collapses of sinkholes and caves [26,29].

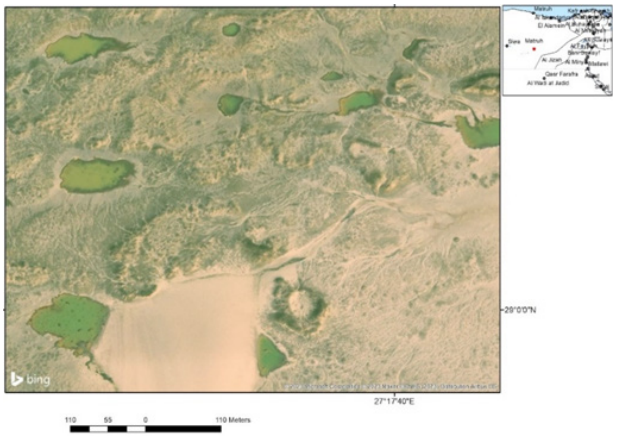

Figure 19. Sinkholes, partly filled with water (green colour) within Eocene limestones in the Western Desert after rare rainfall visible on a Bing Map-scene.

4.6. Potential Impact Craters

Several potential cosmic impact craters in Egypt have been reported in the Earth Impact Database (EID) created by the Planetary and Space Science Centre (PASSC) [30], Canada. Not all of them have been verified so far. However, besides so many volcanic craters with central plugs, it is very difficult to identify impact craters based on remote sensing data (Figure 20). Nevertheless, the potential impact of larger meteorites creating craters has to be considered in a natural hazard database.

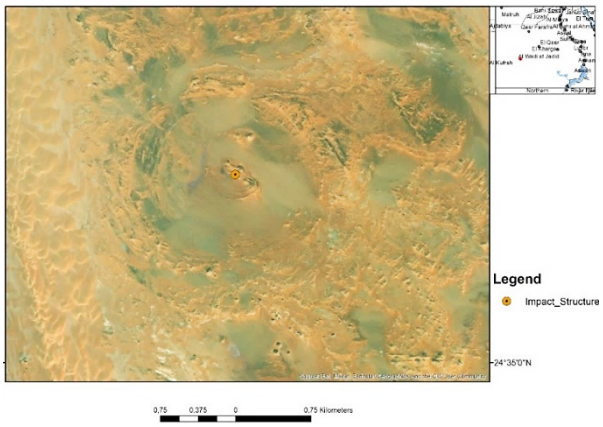

Figure 20. Assumed impact crater visible on a World Imagery scene (implemented in ArcGIS/Copyright© Esri), found in the Earth Impact Database (EID) created by the Planetary and Space Science Centre (PASSC), Canada [30].

5. Discussion

Remote sensing and GIS tools support the systematic detection of ring structures and the gain of additional knowledge related to their complex geologic setting and origin. These tools serve as well to monitor their impact on their environment and on potential geohazards. An overview of the main types of ring structures and their origin could be derived from the evaluations of different satellite data as well as their potential influence on land use.

To analyze the traces of different kinds of geodynamic activity and the areas where these traces occur concentrated, density calculations were carried out in ArcGIS (Figure 21). The density calculation of the digitized larger ring structures, craters, major fault zones and dikes clearly indicates that the southern part of Egypt between the latitudes 22°–25° N is exposed to higher densities of traces of magmatic and geodynamic activity as well as the Red Hills region. By merging the different density calculation results this becomes evident (Figure 21e).

Further on, there are many questions about the impact of ring structures on the environment and on the occurrence of future natural hazards still open, especially considering volcanic activity. Nevertheless, the evaluations of satellites can help to point out where future research could be focused such as in the case of circular and oval shaped structures in Tertiary sedimentary outcrops.

However, whenever underneath the vast dune fields and aeolian covers in large parts of Egypt further remnants of these traces (such as volcanism) are discovered, the density calculations would have to be adapted.

The long-term, aseismic slips and seismic movements along the large, W-E-oriented strike-slip faults in southern Egypt play an important role as the higher distribution densities of ring structures, craters and volcanic cones occur concentrated in the areas of the extended W-E faults. Along these fault systems and zones of weakness, magma could intrude with less hindrance. The question arises whether areas prone to natural hazards in the past will be the same areas affected by hazards in the future.

The evaluation feasibilities of satellite data come to its limits whenever the origin of circular features cannot be determined or they are buried deeper under younger sediments and, thus, are not visible.

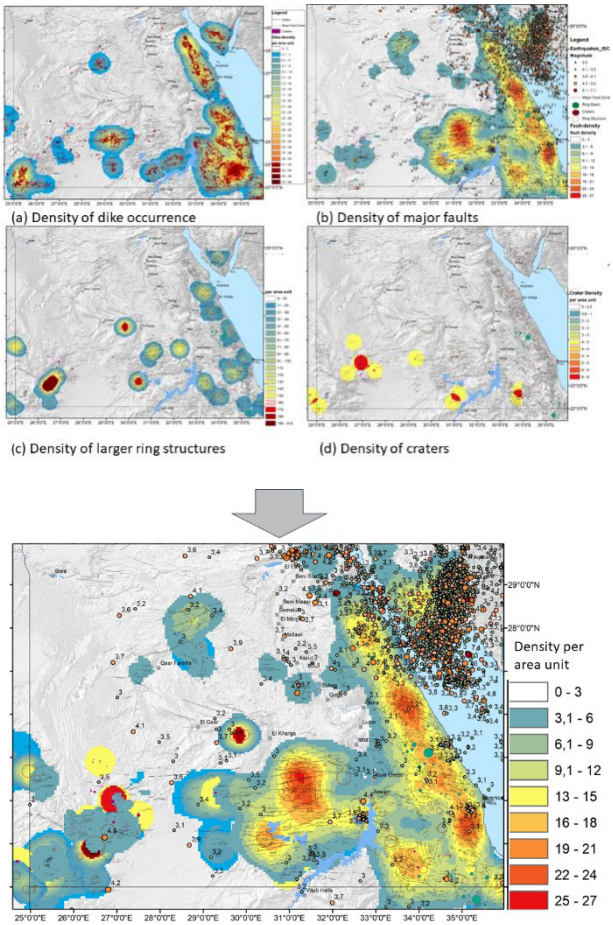

(e) Merging of the different density results.

Figure 21. Density calculations of different traces of geodynamic activity created in ArcMap.

6. Conclusions

Prevention of damage related to natural hazards to human life and infrastructure requires preparedness and mitigation measurements that should be based on a regularly updated, GIS and data mining. A systematic, GIS integrated inventory of different ring structures and their structural setting in Egypt is suggested as part of

such a natural hazard data base that should be subdivided according to their origin and their geologic setting. For example:

- a GIS related to large magmatic bodies;
- a GIS gathering information related to volcanic features (age, lithologic composition, etc.);
- an inventory of circular and oval-shaped structures within sedimentary strata;
- a GIS containing karst information (sinkholes, caves);
- inclusion of earthquake data and macroseismic maps;
- integration of a geodetic database.

All the information should be summarized and integrated into a natural hazard GIS to improve hazard assessment and monitoring [31,32]. The GIS database would track exposure on a wide variety of scales, formats, and levels of detail by aggregating data for risk assessment that can be updated regularly. Of course, such a GIS would require the joint interdisciplinary efforts of many geoscientific institutions and scientists and the maintenance and regular update of data.

Conflict of Interest

The author declares no conflict of interest.

Funding

This work received no external funding.

Acknowledgments

The author thanks Prof. Dr.Barbara Tewksbury/ Department of Geosciences, Hamilton College, Clinton, NY 13323, USA, and Dr.William Bosworth/Apache Egypt Companies for their support and input.

The author is grateful to the Editorial Team/Editorial Office of the Journal *Prevention and Treatment of Natural Disasters,* UK Scientific Publishing Limited, for all their efforts and the careful editing.

References

1. Mazzini, A.; Lupi, M.; Sciarra, A.; Hammed, M.; Schmidt, S.T.; Suessenberger, A. Concentric Structures and Hydrothermal Venting in the Western Desert, Egypt. *Front. Earth Sci.* **2019**, *7*. [CrossRef]
2. Theilen-Willige, B. Remote Sensing and GeoInformation System (GIS) Contribution to the Inventory and Investigation of Dikes in Egypt. *Mediterr. J. Basic Appl. Sci.* **2023**, *7*(3), 60–84. [CrossRef]
3. Farahat, E.S. The Neoproterozoic Kolet Um Kharit bimodal metavolcanic rocks, south Eastern Desert, Egypt: A case of enrichment from plume interaction? *Int. J. Earth Sci.*, **2006**, *95*, 275–287. [CrossRef]
4. Elsaid, M.; Aboelkhair, H.; Dardier, A.; Hermas, E.; Minoru, U. Processing of Multispectral ASTER Data for Mapping Alteration Minerals Zones: As an Aid for Uranium Exploration in Elmissikat-Eleridiya Granites, Central Eastern Desert, Egypt. *Open J. Geol.* **2014**, *8*, (Suppl1: M5), 69–83. [CrossRef]
5. Radwan, A.; Emam, A.; Elshayeb, G.B.; Younis, M.H. Petrogenesis and tectonic Evolution of the Ring Complexes in Southeastern Desert, Egypt: A Case Study from El-Gezira Alkaline Association. *Nucl. Sci. Sci. J.*, **2023**, *12*, 1–23. [CrossRef]
6. Tewksbury, B.J.; Tarabees, E.A.; Mehrtens, C.J. Origin of an extensive network of non-tectonic synclines in Eocene limestones of the Western Desert, Egypt. *J. Afr. Earth Sci.,* **2017**, *136*, 148–167. [CrossRef]
7. Tewksbury, B.J.; Mehrtens, C.J.; Gohlke, S.A.; Tarabees, E.A.; Hogan, J.P. Constraints from Mesozoic siliciclastic cover rocks and satellite image analysis on the slip history of regional E-W faults in the southeast Western Desert, Egypt. *J. Afr. Earth Sci.,* **2017**, *136*, 119–135. [CrossRef]
8. Theilen-Willige, B.; Naouadir, I. Contribution of Remote Sensing and GIS to the Inventory and Analysis of Factors influencing the Development of Karst Features in the Middle Atlas, Morocco. *Eur. J. Environ. Earth Sci.,* **2022**, *3*(6), 1–17. [CrossRef]
9. Zahera, M.A.; Elbarbary, S.; El-Shahat, A.; Mesbah, H.; Embaby, A. Geothermal resources in Egypt integrated with GIS-based analysis. *J. Volcanol. Geotherm. Res.* **2018**, *365*, 1–12. [CrossRef]
10. El-Wardany, R.M.; Jiao, J.; Zoheir, B.; Kumral, M.; Kaya, M.; Abdelnasser, A. Post-Subduction Granite Magmatism and Gold-Sulfide Mineralization in the Abu Zawal (Fatira) Area, Eastern Desert, Egypt. *Minerals*, **2023**, *13*, 489. [CrossRef]
11. United States Geological Survey USGS, Earth Explorer. Available online: https://earthexplorer.usgs.gov/ (accessed from May to September 2023).
12. ESA Copernicus Open Access Hub. Available online: https://scihub.copernicus.eu/dhus/#/home (accessed on 20 September 2023).
13. NASA Earth Data, Alaska Satellite Facility (ASF). JAXA/ METI, satellite data accessed through ASF DAAC. Available online: https://www.asf.alaska.edu/ (accessed from May to September 2023).
14. Arab Nubia Group Blog, GIS, Remote Sensing & General Applications. Available online: https://blog.arabnubia.com/ (accessed in September 2023).
15. Geological Map of Africa—SIGAfrique—1:10,000,000 scale—Bedrock Age, French Geological Survey (BRGM), France (downloaded from the OneGeology portal). Available online: http://portal.onegeology.org/OnegeologyGlobal/ (accessed on 20 September 2023).

16. Shahin, H.A.A.; Masoud, M.S. Geology, Geochemestry and Radioactivity of Gabal Shendib alkaline Ring Complex, Southeastern Desert. Egypt. *Nucl. Sci. Sci. J.,* **2019**, *8*, 17–38. [CrossRef]
17. Saber, E.A.; Ali, M.H.; El-Sheikh, A.A. Magmatism and Related Mineralizations in Wadi Hammad, North Eastern Desert, Egypt. *Sohag J. Sci.* **2023**, *8*(2), 145–155. [CrossRef]
18. Bosworth, W.; Khalil, S.N.; Ligi, M.; Stockli, D.F.; McClay, K.R. Geology of Egypt: The Northern Red Sea. In *The Geology of Egypt;* Hamimi, Z., El-Barkooky, A., Frías, J.M., Fritz, H., El-Rahman, Eds.; Springer: Cham, 2020; pp. 343–373. [CrossRef]
19. Bosworth, W.; Stockli, D.F. Early magmatism in the greater Red Sea rift: timing and significance. *Can. J. Earth Sci.* **2016**, *53*, 1–19. [CrossRef]
20. Mohamed, A.E.A.; El-Hadidy, M.A.; Deif, A.; Abou Elenean, K. Seismic hazard studies in Egypt. *NRIAG J. Astron. Geophys.* **2012**, *1*, 119–140. [CrossRef]
21. Seleem, T.A.; Aboulela, H.A. Seismicity and Geologic Structures Indubitable in Wadi Hagul, North Eastern Desert, Egypt. *Int. J. Geosci.* **2011**, *2*, 55–67. [CrossRef]
22. International Seismological Centre-ISC. Earthquake data. Available online: http://www.isc.ac.uk/iscbulletin/search/catalogue/interactive/ (accessed on 20 September 2023).
23. US Geological Survey (USGS). Earthquake data. Available online: https://earthquake.usgs.gov/earthquakes/search/ (accessed on 14 September 2023).
24. European-Mediterranean Seismological Centre—EMSC, 2023. Earthquake data. Available online: http://www.emsc-csem.org/ (accessed on 20 September 2023).
25. Youssef, A.M. An Enhanced Remote Sensing Procedure for Material Mapping in the Western Desert of Egypt: A Tool for Managing Urban Development. *Nat. Resour. Res.* **2008**, *17*(4), 215–226. [CrossRef]
26. Youssef, A.M.; El-Shater, A.H.; El-Khashab, M.H.; El-Haddad, B.A. Coupling of field investigations and remote sensing data for karst hazards in Egypt: case study around the Sohag City. *Arab. J. Geosci.* **2017**, *10*, 235. [CrossRef]
27. El Aref, M.; Salama, A.; Hammed, M. Morphotectonic Evolution of Qaret El Sheikh Abdallah Depressions and Denuded Paleo-Karst in the White Desert, El Bahariya-Farafra Karst Territory, Egypt. *Egypt. J. Geo*. **2021**, *65*, 27–53. [CrossRef]
28. Abidi, A.; Demehati, A.; Banouni, H.; El Qandil, M. The importance of underground cavities detection in the choice of constructible areas: case of the Agglomeration of Fez (Morocco). *Geotech. Geol. Eng.,* **2018**, *36*(3), 1919–1932.
29. Abd El Aal, A.K.; Nabawy, B.S.; Aqeel, A.; Abidi, A. Geohazards assessment of the karstified limestone cliffs for safe urban constructions, Sohag, West Nile Valley, Egypt. *J. Afr. Earth Sci.* **2020**, *161*, 103671. [CrossRef]
30. The Earth Impact Database (EID) created by the Planetary and Space Science Centre (PASSC), Canada, African Impact Structures. Available online: http://www.passc.net/EarthImpactDatabase/New%20website_05-2018/Africa.html (accessed on 20 September 2023).
31. Training Package on National Scale Multi-Hazard Risk Assessment, Theory Book PPRD-EAST. Available online: https://www.academia.edu/30308280/Training_Package_on_National_Scale_Multi_Hazard_Risk_Assessment_National_Scale_Multi_Hazard_Risk_Assessment_Theory_Book?email_work_card=view-paper (accessed on 20 September 2023).
32. Khedr, M.Z.; Abo Khashaba, S.M.; El-Shibiny, N.H.; Takazawa, E.; Hassan, S.M.; Azer, M.K.; Whattam, S.A.; El-Arafy, R.A.; Ichiyama, Y. Integration of remote sensing and geochemical data to characterize mineralized A-type granites, Egypt: implications for origin and concentration of rare metals. *Int. J. Earth Sci.* **2023**, 1–29. [CrossRef]